

See discussions, stats, and author profiles for this publication at: <http://www.researchgate.net/publication/23933063>

Electrocorticographic Interictal Spike Removal via Denoising Source Separation for Improved Neuroprosthesis Control

CONFERENCE PAPER *in* CONFERENCE PROCEEDINGS: ... ANNUAL INTERNATIONAL CONFERENCE OF THE IEEE ENGINEERING IN MEDICINE AND BIOLOGY SOCIETY. IEEE ENGINEERING IN MEDICINE AND BIOLOGY SOCIETY. CONFERENCE · FEBRUARY 2008

DOI: 10.1109/IEMBS.2008.4650392 · Source: PubMed

CITATION

1

DOWNLOADS

16

VIEWS

87

3 AUTHORS:



[Aysegul Gunduz](#)

University of Florida

31 PUBLICATIONS 221 CITATIONS

SEE PROFILE



[Justin C. Sanchez](#)

DARPA

165 PUBLICATIONS 1,362 CITATIONS

SEE PROFILE



[Jose C Principe](#)

University of Florida

907 PUBLICATIONS 9,437 CITATIONS

SEE PROFILE

Electrocorticographic Interictal Spike Removal via Denoising Source Separation for Improved Neuroprosthesis Control

Aysegul Gunduz, Justin C. Sanchez, and Jose C. Principe

Abstract—Electrocorticographic (ECoG) neuroprosthesis is a promising area of research that could provide channels of communication and control for patients who have lost their motor functions due to damage to the nervous system. However, implantation of subdural electrodes are clinically restricted to diagnostics of pre-surgical epileptic patients. Hence, interictal activity is present in the recordings across various areas of the sensorimotor cortex and suppresses the amplitude modulated features extracted to model hand trajectories. Denoising source separation is a recently introduced framework which extracts hidden structures of interest within the data through denoising the source estimates with filters designed around prior knowledge on the observations. Herein, we exploit the high amplitude quasiperiodic nature of the observed interictal spikes and show that removal of the interictal activity improves linear prediction of hand trajectories.

I. INTRODUCTION

Brain machine interfaces (BMIs) offer new rehabilitation options to patients who have lost their motor capability through decoding motor intent directly from the sensorimotor cortex. Recent focus has been given to electrocorticographic (ECoG) BMIs [1], [2], [3] due to higher signal amplitudes with increased spectral and spatial resolution compared to scalp electrode recordings (EEG), and clinical implant viability of subdural electrodes in human patients as opposed to intracortical micro-electrode arrays. Amplitude modulation of ECoG rhythms have been found to continuously map motor behavior in one and two-dimensional experiments [1], [2], [3], [4].

Since implantation of subdural electrodes in human patients is limited to patients seeking epilepsy surgery, one must consider that the abnormal activity of epileptic tissue could influence motor decoding. In the BMI literature, the seizure onset zone of the subjects participating in BMI studies are remote from the primary motor cortex, however, interictal spiking activity can be present in the global sensorimotor system. The presence of interictal spikes is observed as non-stationary high amplitude discharges and could potentially corrupt the amplitude modulated motor features.

To contend with this problem, independent component analysis (ICA) [5] has been proposed to localize and separate

interictal sources from background EEG [6] and MEG [7]. *Denoising source separation* (DSS) is a recently introduced framework [8] which relaxes the independence assumption of the components to uncorrelatedness and isolates sources with desired structures [9]. The algorithm makes use of a priori knowledge or inspection of data to iteratively extract desired structures through *denoising functions*. Each source is extracted separately (one component at a time) and thus different patterns of interest can be isolated for each source. Hence, the algorithm is more efficient and exploitative compared to ICA. In this paper, we explore and isolate ECoG interictal spiking activity via DSS and study the amplitude modulated motor features in the “corrected” channels after the removal of the epileptogenic sources.

II. MATERIALS AND METHODS

A. Data Collection and Experimental Setup

The patient volunteering in this study was undergoing extraoperative subdural grid electroencephalographic monitoring for the treatment of intractable complex partial epilepsy at Shands Hospital, University of Florida. The experimental paradigms were approved by the Institutional Review Boards. The grid consisted of a 1.5mm thick silastic sheet embedded with platinum-iridium electrodes (4mm diameter with 2.3mm diameter exposed surface) spaced at 1cm center-to-center distances. The primary motor cortex was determined by direct electrical stimulation of the subdural grids.

The patient was cued to follow a predefined cursor trajectory presented on an LCD screen with an active area of 20cm x 30cm with her index finger while neuronal modulations from the implanted ECoG electrodes were simultaneously being recorded. The paradigm consisted of a widely performed center-out task and a target selection task. Subdural potentials from 32 channels were recorded at a sampling frequency of 12kHz whilst the patient was engaged in the behavioral task. The potentials were bandpass filtered from 1Hz to 6kHz while behavioral trajectory recordings were stored with a shared time clock and sampled at 381.5 Hz.

Our goal is to extract amplitude modulated features from the ECoG recordings to map the hand trajectories for further information). Spectrally preprocessed cortical recordings have been shown to correlate with motor tasks in frequency bands comprised of slow potentials (1-60Hz), the gamma band (60-100Hz), fast gamma band (100-300Hz) and ensemble depolarization (300-6kHz) [1]. We define the band specific amplitude modulated control features, as the integrated power of the ECoG rhythm in non-overlapping bins of 100 msec. These features from all channels form the

This work was supported in part by DARPA under grant ONR-450595112, the National Science Foundation under Grant #CNS-0540304 and the Children’s Miracle Network.

A. Gunduz, and J.C. Principe are with the Computational NeuroEngineering Laboratory at the Department of Electrical and Computer Engineering, University of Florida, Gainesville, FL 32611 (e-mail: {aysegul, principe}@cnel.ufl.edu).

J.C. Sanchez is with the Neuroprosthesis Research Group at the Department of Pediatrics, University of Florida, Gainesville, FL 32610 (e-mail: jcs77@ufl.edu).

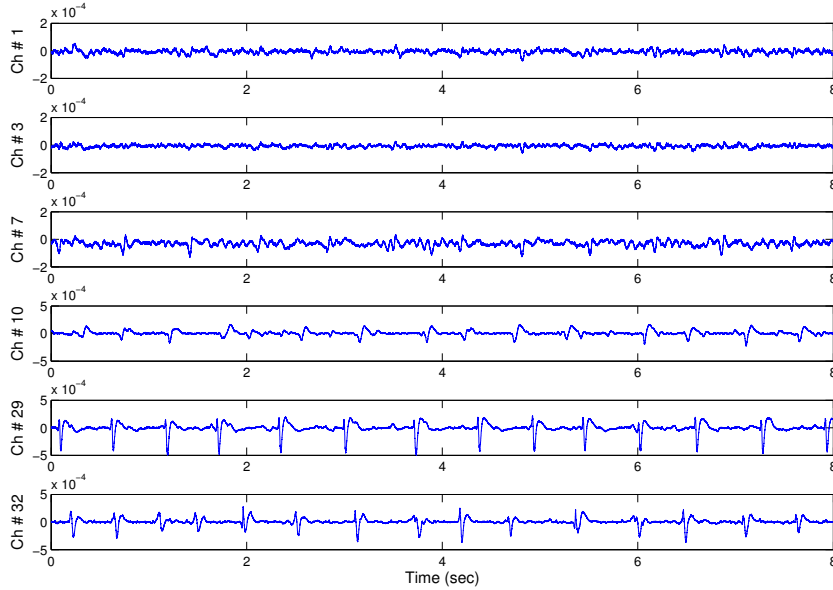


Fig. 1. Representative channels of ECoG activity recorded during BMI behavioral experiments. The top three channels show only slight contamination of interictal activity. These channels contribute to the reconstruction of the hand trajectories. The bottom three channels show high amplitude quasiperiodic interictal discharges which suppress the features modulating the hand movement.

inputs to Wiener filters through which hand trajectories are reconstructed. The hand trajectories are downsampled to 10 Hz to match the sampling frequency of the power features.

Representative channels of the collected ECoG activity is presented in Figure 1. The first three rows correspond to channels that are not dominated by interictal activity. Modulations in these channels have been found to contribute to the prediction of hand position in Wiener sensitivity analysis in ensemble activity (refer to [1] for details). The amplitude modulated motor features extracted from Channel # 1 (Figure 1- top row) in the spectral range of 300Hz-6kHz are superimposed on the vertical hand position in Figure 2a (both signalized normalized to unit variance to emphasize correlation). The bottom three channels, however, are heavily contaminated with high amplitude quasiperiodic interictal spikes. The reconstructed hand trajectory is less sensitive to these channels. Moreover, if initial channel selection is not performed, these channels add noise to the inputs of the models. The same features used in the prediction of the vertical hand position are depicted in Figure 2b for Channel # 32 (Figure 1-bottom row). The activity modulating the hand behavior is suppressed by the power in the interictal spikes. In the following subsections we present the DSS algorithm and the denoising function used for the removal of the quasiperiodic interictal activity.

B. Denoising Source Separation

DSS is a semiblind source separation algorithm based on the linear mixing assumption of hidden sources:

$$\mathbf{X} = \mathbf{A}\mathbf{S} + \mathbf{v}, \quad (1)$$

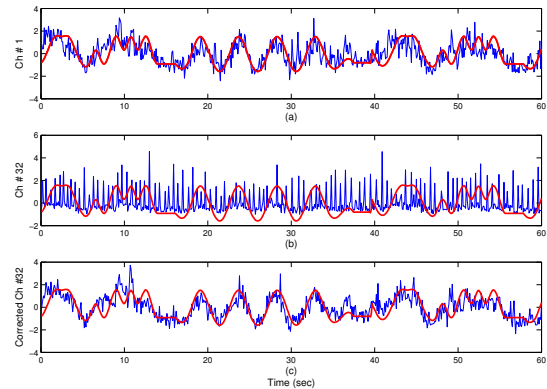


Fig. 2. The amplitude modulated features extracted from ensemble activity superimposed on vertical hand position. (a) The features extracted from Channel # 1 are highly correlated with the hand trajectory, whereas (b) the power in the interictal spikes are dominating the features in Channel # 32. (c) The features extracted from Channel # 32 after the DSS-based interictal spike removal.

where the observation matrix, \mathbf{X} , consists of M measurements recorded over the observation time $t = 1, \dots, T$. These measurements are assumed to be linear combinations of N sources, denoted by the source matrix \mathbf{S} , collected under Gaussian noise, \mathbf{v} . If the measurements are collected through spatial sensors, the mixing matrix \mathbf{A} yields the spatial patterns of the sources. This formulation is common to all linear source separation algorithms [8]. Unlike blind source separation methodologies, DSS exploits prior knowledge

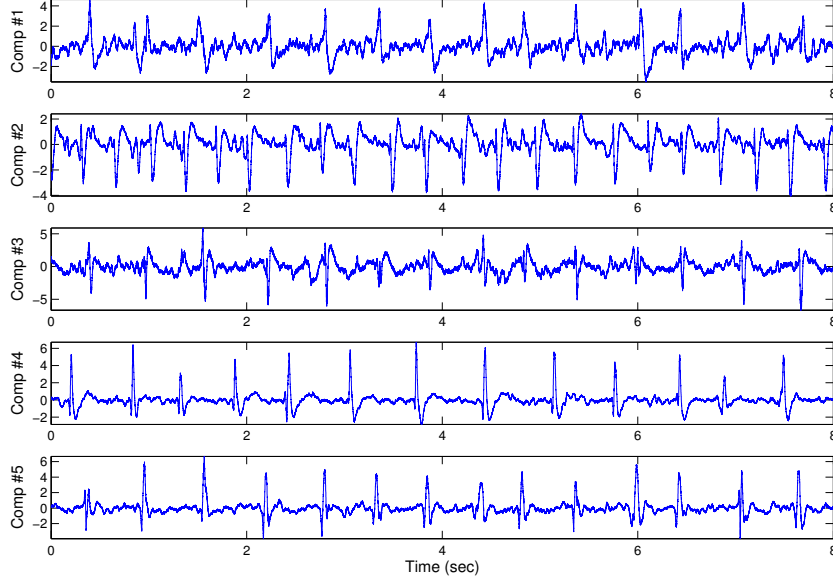


Fig. 3. The extracted interictal spikes via threshold localization and denoising averaging.

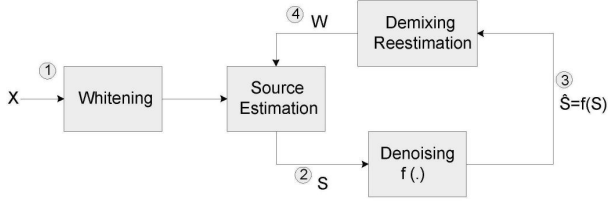


Fig. 4. Block diagram of the iterative DSS algorithm.

about the sources to extract desired structures within the data (e.g. non-Gaussianity, spectral content, general shape patterns etc.). This is achieved by iteratively filtering the current source estimates through *denoising functions* chosen to emphasize and maximize the desired properties in current source estimates. In the DSS framework sources are extracted one component at a time, s_i , allowing different denoising functions to be employed for the extraction of other desired structures. The algorithm consists of four successive steps [9]:

- 1) Demeaning and whitening the data through eigenvalue decomposition.
- 2) Source estimation by demixing the data:

$$\mathbf{s}_i = \mathbf{w}_i^T \mathbf{X}, \quad (2)$$

where \mathbf{w}_i is a column of the demixing matrix. In order to assure that the sources extracted from the whitened data are uncorrelated, \mathbf{W} is restricted to be orthogonal. This orthogonal projection of whitened data also yields

sources with unit covariance.

- 3) Denoising the source estimates:

$$\hat{\mathbf{s}}_i = \mathbf{f}(\mathbf{s}_i) \quad (3)$$

$\mathbf{f}(\cdot)$ is the denoising function which is chosen to gradually maximize the desired properties on the source estimate. Denoising functions can be linear or nonlinear to utilize the prior information on the data.

- 4) Reestimation and orthogonalization of the demixing matrix:

$$\mathbf{w}_i = \mathbf{X} \hat{\mathbf{s}}_i^T \quad (4)$$

The reestimated demixing vector is orthogonalized to the previously found columns of \mathbf{W} through Gram-Schmidt orthogonalization [5].

Steps 2-4 are iterated for each source estimate until the angle between the previous and current demixing estimates is less than a preset threshold, ϵ or when the maximum number of iterations is reached. The algorithm is summarized in Figure 4.

C. DSS for Quasiperiodic Interictal Spike Removal

Herein, we exploit the quasiperiodic nature of the observed interictal spikes¹. Sarela [8] suggested averaging across the repetitious periods of the quasiperiodic data in order to increase SNR on the source estimate. The spikes are localized through simple thresholding mechanisms in the initial source estimates. Each peak-to-peak period is dilated to the same length and are averaged. The denoised signal estimate is found by replacing the averaged period into

¹We should point out that this quasiperiodicity is specific to this Patient and that this property is not a global property of ECoG interictal spikes.

the original periods. This whole averaging process is the “denoising function” applied to the source estimates.

In this study, the initial thresholding was applied to the channels and spikes in the heavily dominated channels were detected. These time stamps were used as the first references in the averaging denoising function. The interspike intervals on the source estimates were dilated and spike triggered averaging was performed. This denoising process increased the interictal activity-to-background activity ratio. Figure 3 depicts the extracted quasiperiodic interictal sources on a dataset of 1 minute. The corrected channels were attained by removing the interictal components:

$$\mathbf{X}_{corr} = \mathbf{X} - \sum_{i=1}^5 \mathbf{a}_i^T \mathbf{s}_i \quad (5)$$

The amplitude modulated features extracted from the corrected channels in the 300Hz-6kHz spectral band are given in Figure 2c and the increase in correlation with the vertical hand position is evident as compared to Figure 2b.

D. Modelling Motor Behavior Through Denoised Channels

Wiener filters model the hand position through a linearly weighted short-term history (tap delay line) of the power modulation in these bands. The features extracted from the high frequency ensemble depolarization activity (300Hz - 6kHz) yielded the best reconstruction before [1] and after the removal of the interictal spikes. The performance results on with the original channels and the denoised channels as inputs to a Wiener filter of order 25, which yields a tap delay line of 2.5 secs, are summarized in Table 1 (for further details on the Wiener filter model and parameters please refer to [1]). The correlation coefficients (CC) and normalized mean squared errors (MSE) between the vertical hand position and the filter outputs computed on nonoverlapping windows of 5 secs are given in Table 1. The CCs are computed by normalizing the cross-correlation between the filter outputs and desired trajectories in each 5 sec window by their individual standard deviations. The normalized MSEs are computed by dividing the power of the error in each 5 sec window by the power of the desired signal in that window.

The removal of the interictal activity improved the mean of both performance criteria (increased CC and lowered MSE). Still, due to the high variance in the results, the significance of the improvement in both measures are further verified via paired t-tests, which statistically test the hypothesis that the results attained via the original and denoised signals come from distributions with equal means. The hypotheses that the CCs and MSEs attained via the original signals and the denoised signals came from distributions of the same mean were both rejected at a significance level $\alpha = 0.05$. The low p-values of the t-tests are also provided in Table 1.

III. DISCUSSION

In this study we presented an interictal spike removal methodology based on denoising source separation. Unlike other blind source separation techniques (such as ICA), we did not have to perform the simultaneous extraction of all

TABLE I
WIENER FILTER RESULTS

	Original Channels	Corrected Channels	p-value of paired t-test
Correlation coefficient	0.60 ± 0.25	0.68 ± 0.20	4.31e-15
Mean Squared Error	0.88 ± 0.52	0.64 ± 0.37	2.88e-14

thirty two components (which is computationally extensive) and then study which components consisted of interictal activity. Instead, we exploited the observed quasiperiodic nature of the interictal spikes. Channels with high amplitude discharges were detected by simple thresholding mechanisms and these localizations were used for the extraction of the components given in Figure 3 which reduced computational costs. The spatially weighted components were subtracted from the ECoG measurements and not only were the highly dominated channels were corrected but also the low amplitude propagation of the interictal activity to the neighboring channels were suppressed. The removal of the interictal spikes improved the performance of the models mapping the amplitude modulated ECoG features to the hand trajectories. Future studies will include using DSS for the extraction of ECoG features that can be directly used in BMIs for the prediction of hand trajectories.

REFERENCES

- [1] J.C. Sanchez, A. Gunduz, J.C. Principe, and P.R. Carney, “Extraction and Localization of Mesoscopic Motor Control Signals for Human ECoG Neuroprosthetics”, *Journal of Neuroscience Methods*, vol. 167, pp. 63-81, 2008.
- [2] T. Pistohl, T. Ball, A. Schulze-Bonhage, A. Aertsen, and C. Mehring, “Prediction of arm movement trajectories from ECoG-recordings in humans”, *Journal of Neuroscience Methods*, vol. 167, pp. 105-114, 2008.
- [3] G. Schalk, J. Kubanek, K.J. Miller, N.R. Anderson, E.C. Leuthardt, J.G. Ojemann, D. Limbrick, D. Moran, L.A. Gerhardt, and J.R. Wolpaw, *Journal of Neural Engineering*, vol. 4, pp. 264-275, 2007.
- [4] E.C. Leuthardt, G. Schalk, J.R. Wolpaw, J.G. Ojemann, and D. Moran, “A brain-computer interface using electrocorticographical signals in humans”, *Journal of Neural Engineering*, vol. 1, pp. 63-71, 2004.
- [5] A. Hyvarinen, J. Karhunen, and E. Oja, *Independent Component Analysis*, John Wiley, 2001.
- [6] K. Kobayashi, C.J. James, T. Nakahori, T. Akiyama, and J. Gotman, “Isolation of epileptiform discharges from unaveraged EEG by independent component analysis”, *Clinical Neurophysiology*, vol. 110, pp. 1755-1763, 1999.
- [7] A. Ossadtchi, S. Baillet, J.C. Mosher, D. Thyerlei, W. Sutherling, R.M. Leahy, “Automated Interictal Spike Detection and Source Localization in MEG using ICA and Spatio-Temporal Clustering”, *Clinical Neurophysiology*, vol. 115, pp. 508-522, 2004.
- [8] J. Sarela and H. Valpola, “Denoising Source Separation”, *Journal of Machine Learning Research*, vol.6, pp. 233-272, 2005.
- [9] A. Ilin, H. Valpola and E. Oja, “Explatory analysis of climate data using source separation methods”, *Neural Networks*, vol. 19, pp. 155-167, 2006.